International Journal of Thermophysics, Vol. 15, No. 1, 1994

The Transport Properties of Ethane. I. Viscosity

S. Hendl,[1] J. Millat,[2] E. Vogel,[1] V. Vesovic,[3] W. A. Wakeham,[3] J. Luettmer-Strathmann,[4] J. V. Sengers,[4] and M. J. Assael[5]

Received July 1, 1993

A new representation of the viscosity of ethane is presented. The representative equations are based upon a body of experimental data that have been critically assessed for internal consistency and for agreement with theory in the zero-density limit, vapor phase, and critical region. The representation extends over the temperature range from 100 K to the critical temperature in the liquid phase and from 200 K to the critical temperature in the vapor phase. In the supercritical region, the temperature range extends to 1000 K for pressures up to 2 MPa and to 500 K for pressures up to 60 MPa. The ascribed accuracy of the representation varies according to the thermodynamic state from $\pm 0.5\%$ for the viscosity of the dilute gas near room temperature to $\pm 3.0\%$ for the viscosity at high pressures and temperatures. Tables of the viscosity, generated by the relevant equations, at selected temperatures and pressures and along the saturation line, are also provided.

KEY WORDS: ethane; *n*-alkanes; transport properties; viscosity.

1. INTRODUCTION

Recent developments of software packages for process design and their subsequent, widespread use have generated a great deal of activity in a number of chemical-engineering fields. Such design packages invariably require the thermophysical properties of different process streams and recent tests have indicated that the accuracy of thermophysical properties

[1] Fachbereich Chemie, Universität Rostock, D-18051 Rostock, Germany.
[2] TECHRO e. V., Platz der Freundschaft 1, D-18059 Rostock, Germany.
[3] IUPAC Transport Properties Project Center, Department of Chemical Engineering and Chemical Technology, Imperial College, London SW7 2BY, United Kingdom.
[4] Institute for Physical Science and Technology, University of Maryland, College Park, Maryland 20742, U.S.A.
[5] Faculty of Chemical Engineering, Aristotle University, 54006 Thessaloniki, Greece.

0195-928X/94/0100-0001$07.00/0

are of paramount importance [1]. Thus, research and development of state-of-the-art representations of thermophysical properties as functions of temperature and pressure have gained renewed momentum. Under the auspices of IUPAC, a research program has been initiated to develop representations of the transport properties of industrially important fluids. The basic philosophy of the program is to make use of the best available experimental data, selected on the basis of a critical analysis of the methods of measurement. This information is complemented with guidance available from theory to produce accurate, consistent, and theoretically sound representations of the transport properties over the widest range of thermodynamic states possible. The first fluid studied in this program was carbon dioxide [2], and we now present the results for ethane. The present paper deals with viscosity, while the results for thermal conductivity are presented in the following paper, part II.

A number of correlations of the viscosity of ethane, based on comprehensive reviews of the data available at the time, were published in the seventies [3–5]. Since then, new experimental measurements have been performed and our understanding of the theory of transport properties has improved considerably. In the late eighties two more correlations were published [6, 7]. Unfortunately, the accuracy and usefulness of either of them are very difficult to judge because little indication of the development of the viscosity correlation was given. Specifically, either no critical analysis of the experimental data was undertaken [6] or no description of the data selected as a basis for the correlation was presented [7]. Recently a new, critical evaluation of the available data for viscosity of ethane has been carried out [8]. The resulting representation covers a wide range of thermodynamic states. Nevertheless, it was felt that, owing to the developments in the last 2 years, improvements are already possible in certain regions of the thermodynamic space. First, new viscosity data became available at low and high temperatures in the low-density range [9, 10] which, as our subsequent analysis shows, greatly improve the viscosity correlation in that region. Second, a novel way of predicting and correlating the data in the vapor phase at low densities has been developed [11] and incorporated in the present correlation. Third, in practice equations for transport properties need to be used in conjunction with satisfactory equations of state; for ethane a nonclassical equation of state valid in an appreciable range around the critical point is now available [12]. Finally, in order to analyze the thermal-conductivity data which are the subject of part II, a representation of the viscosity which is as accurate and as self-consistent as possible is essential.

The following sections briefly summarize the theory and procedures used to develop the representation of the viscosity of ethane as well as

presenting the coefficients and functional forms of the resulting correlation. Since some of the methodology is the same as that used in our earlier work, the reader is referred to the publication on carbon dioxide for further details [2].

2. METHOD

It is customary [2, 13], for both fundamental and practical reasons, to decompose the viscosity, $\eta(\rho, T)$, of the fluid as a function of the density, ρ, and the temperature, T, into the sum of three contributions,

$$\eta(\rho, T) = \eta_0(T) + \Delta\eta(\rho, T) + \Delta_c\eta(\rho, T) = \bar{\eta}(\rho, T) + \Delta_c\eta(\rho, T) \qquad (1)$$

Here η_0 is the viscosity in the zero-density limit, $\Delta\eta$ an excess viscosity, and $\Delta_c\eta$ a critical enhancement. It is also useful to define the background contribution $\bar{\eta}$ as the sum of the first two terms in Eq. (1). The advantage of this approach, in the development of the viscosity correlation, is that it is possible to use both theoretical and experimental information to treat some of the contributions independently. Thus, it is possible to examine some of the available experimental data in the light of the most modern theory and to confirm the internal consistency of various sets of experimental data. Furthermore, in the zero-density limit and around the critical point, theoretical studies have suggested acceptable functional forms for the representation of experimental data [2, 14].

In order to perform such an analysis one must make use of experimental data over as wide a range of thermodynamic states as possible. Appendix I (Table AI) lists all the sources of data on the viscosity of ethane [9, 10, 15–46] and indicates the range covered and the method of measurement for each publication. A critical analysis of all these data has been undertaken to define the primary data sets for each contribution to Eq. (1). Ideally, the primary data set comprises those measurements performed in instruments for which a full working equation exists and for which a high precision in measuring the viscosity has been achieved. In practice, these constraints have to be relaxed in order to cover as much as possible of the phase space by including other data. Generally, it is legitimate to include only those data with a well-defined uncertainty level which cannot be demonstrated to be inconsistent with other data or with theory.

For the purposes of the analysis the experimental viscosity data must be available at specified temperatures and densities. The measurements are usually performed at specific temperatures, T, and pressures, P. In order to be entirely consistent it is necessary to evaluate the density of the fluid from the temperature and pressure reported by experimentalists by the use

of a single equation of state (EOS). For this purpose we have employed the most recent classical EOS for ethane outside the critical region [8] and a new parametric crossover EOS in the critical region [12]. The switching between the two EOS has been performed along the rectangular boundary in the temperature-density plane given by $302.5\ \mathrm{K} \leqslant T \leqslant 316\ \mathrm{K}$, $3.82\ \mathrm{mol \cdot L^{-1}} \leqslant \rho \leqslant 8.65\ \mathrm{mol \cdot L^{-1}}$ [12].

In subsequent sections we treat each contribution separately analyzing the primary data using the best available theoretical guidance. The independent representations are then developed for each term in Eq. (1), which, when combined, give the global correlation for the viscosity of ethane over a wide range of temperature and pressure. Throughout this work the temperature is in units of Kelvin in terms of IPTS-68, the pressure in units of MPa, the density in units of $\mathrm{mol \cdot L^{-1}}$, and the viscosity in units of $\mu\mathrm{Pa \cdot s}$.

3. THE ZERO-DENSITY LIMIT

The viscosity of a fluid in the zero-density limit, η_0, is an experimentally accessible quantity so that it is possible to analyze η_0 independently of other terms in Eq. (1) [47, 48]. Furthermore, the existence of a well-developed kinetic theory [49] in the same limit gives some guidance as to the form of the correlation. Thus, it would seem that the zero-density limit is a natural starting point for the development of any viscosity correlation.

An analysis of the zero-density viscosity data was recently performed [50], and since no new experimental measurements have been carried out in the interim, a short recapitulation of the earlier correlation is all that is necessary here. The kinetic theory of dilute gases relates the viscosity of a pure gas to an effective collision cross section which contains all the dynamical and statistical information about the binary collisions. In a practical engineering form, the viscosity in the zero-density limit is given by

$$\eta_0(T) = \frac{0.021357[TM]^{1/2}}{\sigma^2 \Omega_\eta^*} \tag{2}$$

where Ω_η^* is the reduced effective collision cross section, T is the temperature in Kelvin, M is the relative molecular mass, σ is a length scaling parameter in nm, and η_0 is in units of $\mu\mathrm{Pa \cdot s}$. The numerical constant in Eq. (2) was obtained by the use of the recommended values of fundamental constants [51].

In developing the viscosity correlation, experimental values of Ω_η ($\Omega_\eta = \pi\sigma^2\Omega_\eta^*$) have been derived from each of the various primary data

sources, which are listed in Ref. 50. Then the complete set of primary data for $\Theta_\eta^*(T^*)$ was fitted, by the use of appropriate statistical weights, to the functional form

$$\ln \Theta_\eta^* = \sum_{i=0}^{n} a_i (\ln T^*)^i \tag{3}$$

where the reduced temperature T^* is given by

$$T^* = kT/\varepsilon \tag{4}$$

and ε/k is an energy scaling parameter in Kelvin.

It has been found that the experimental viscosity data for ethane can be represented, within their estimated experimental uncertainty, by means of Eqs. (2) and (3) by the use of the coefficients a_i from a "universal" correlation [52, 53]. The advantage of this fortuitous finding is that the resulting correlation can be safely extrapolated to an upper temperature limit of $T = 1000$ K, although the actual highest experimental data point is at $T = 633$ K. This upper limit represents a reasonable limit at which the properties of gaseous ethane might be required in practical applications. Table I contains all the relevant coefficients for the representation of the zero-density viscosity of ethane. The resulting correlation [50] is valid in the temperature range from 200 to 1000 K, and its uncertainty is estimated to be $\pm 0.5\%$ in the range $300\ \text{K} \leqslant T \leqslant 600\ \text{K}$, increasing to ± 1.5 and $\pm 2.5\%$ at 200 and 1000 K, respectively.

4. THE CRITICAL REGION

The viscosity of a pure fluid shows a weak enhancement in a small region around the critical point and becomes infinite at the critical point [54]. The actual range of temperatures and densities where a critical

Table I. Coefficients for the Representation of the Effective Collision Cross Section of Ethane, Eq. (3)[a]

i	a_i
0	0.221 882
1	−0.507 9322
2	0.128 5776
3	−0.008 32817
4	−0.002 71317

[a] $\varepsilon/k = 264.70$ K; $\sigma = 0.43075$ nm; $M = 30.069$.

enhancement in viscosity is observed is quite small. For instance, at the critical density $\rho = \rho_c$ the critical viscosity enhancement exceeds 1% of the background only at temperatures within 6 K from the critical temperature. Nevertheless, the critical enhancement has been observed experimentally for a number of fluids [43, 55–59] and its existence has been clearly established.

Unlike the viscosity, the thermal conductivity exhibits a critical enhancement in a large range of temperatures and densities around the critical point [54]. A theoretical approach for dealing with the critical enhancement of the transport properties has been developed by Olchowy and Sengers [60]. Since the critical-enhancement effect is very important in developing a quantitative representation of the thermal conductivity, we postpone an explanation of this theoretical approach to part II. For the analysis of the small critical viscosity enhancement in the present paper, it is sufficient to quote only the resulting equations.

The critical viscosity enhancement, $\Delta_c\eta$, in Eq. (1) is represented by an equation of the form [14, 61]

$$\Delta_c\eta = \bar{\eta}[\exp(zH) - 1] \tag{5}$$

where H is a crossover function specified in Appendix II and where z is a critical exponent [59, 62–64] given in Table II. The crossover function H

Table II. Constants in the Equations for the Critical Viscosity Enhancement

Critical parameters	
T_c	305.33 K
P_c	4.8718 MPa
ρ_c	6.87 mol · L^{-1}
Critical exponents	
z	0.063
ν	0.63
γ	1.239
Critical amplitudes	
R	1.03
ξ_0	0.19 nm
Γ	0.0541
Cutoff wavenumber	
q_D^{-1}	0.187 nm

depends on the thermodynamic properties of the fluid, which in turn are calculated from the available EOS as specified in Section 2. In addition, the crossover function H depends on the background contributions $\bar{\eta}$ and $\bar{\lambda}$ to the viscosity and to the thermal conductivity, the correlation length ξ, and a system-dependent parameter q_D, which represents a large wave-number cutoff for the critical fluctuations. The correlation length ξ is, in practice, calculated from a dimensionless susceptibility $\bar{\chi}$ defined as

$$\bar{\chi} = \rho(\partial\rho/\partial P)_T P_c \rho_c^{-2} \tag{6}$$

where P_c is the critical pressure. Specifically we use

$$\xi = \xi_0(\Delta_c\bar{\chi}/\Gamma)^{\nu/\gamma} \tag{7}$$

with

$$\Delta_c\bar{\chi} = \bar{\chi}(T, \rho) - \bar{\chi}(T_r, \rho)\frac{T_r}{T} \tag{8}$$

Here ν and γ are universal critical exponents, ξ_0 and Γ are system-dependent critical amplitudes that can be calculated from the asymptotic critical behavior of the EOS, and $T_r = 1.5T_c$ is a suitably chosen reference temperature far away from the critical temperature T_c [14, 61]. The cutoff parameter q_D is determined from an analysis of experimental information for the critical enhancement in the thermal conductivity as discussed in part II. The values of all the relevant constants entering the description of the critical enhancement of the viscosity, Eqs. (5) and (8), are given in Table II.

Detailed experimental studies of the viscosity of ethane in the critical region have been reported by Iwasaki and Takahashi [43], who measured the viscosity and the density simultaneously as a function of pressure along four near-critical isotherms. We have accepted the experimental densities reported by Iwasaki and Takahashi [43]. These values depart considerably from those that we would calculate using our EOS [8, 12] from their reported temperatures and pressures. As in the case of carbon dioxide, we assume that there is an error in the pressures reported.

Evidently, a comparison of the predicted critical enhancement of the viscosity of ethane with experimental data requires separation of the term $\Delta_c\eta$ from the experimental viscosity data. In practice, it is difficult to perform this separation unequivocally. Thus we have adopted, as before [2], an iterative approach in which a background viscosity is postulated on the basis of the data available in regions where the critical enhancement is negligible. In practice, as our work on carbon dioxide has shown [2], if

one starts with such a background viscosity, only a very small subsequent refinement is necessary. Here we use a background viscosity evaluated as described above to determine the critical enhancement of the viscosity of Iwasaki and Takahashi's data by subtracting $\bar{\eta}$ from their experimental viscosities according to Eq. (1). The results are shown in Fig. 1, where the predicted enhancement is shown as the solid line for four near-critical isotherms, while the points represent the experimental data. The uncertainty claimed for the viscosity measurements of Iwasaki and Takahashi implies an uncertainty in the critical enhancement of $\pm 0.5\ \mu\text{Pa} \cdot \text{s}$. It can be seen that, whereas some features of the enhancement are reproduced moderately well, there are large systematic deviations beyond the level of experimental uncertainty at densities below the critical density and, especially, around $4.0\ \text{mol} \cdot \text{L}^{-1}$, where the critical enhancement is expected to be small.

It is therefore necessary to examine the comparison with the data of Iwasaki and Takahashi [43] in more detail to establish the possible reason for this discrepancy. Noting the similar shape of the experimental results along the four isotherms in Fig. 1, we think it is plausible to assert that the background postulated in this region of densities is incorrect. One can therefore deduce a "local" background viscosity from the data of Iwasaki and Takahashi [43] alone, utilizing their results at temperatures away

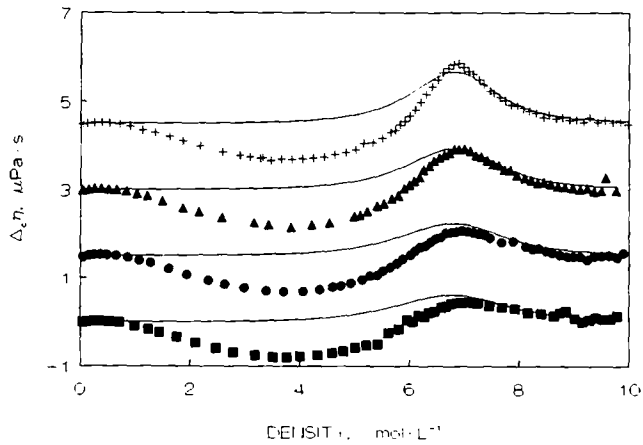

Fig. 1. The critical enhancement of the viscosity deduced from the data of Iwasaki and Takahashi [43] by the use of a "global" background viscosity: +, $T = 305.65$ K; ▲, $T = 305.85$ K; ●, $T = 306.15$ K; ■, $T = 306.45$ K. The solid lines represent the values calculated from Eq. (5). To separate the isotherms the viscosity values have been displaced by $1.5\ \mu\text{Pa} \cdot \text{s}$ each.

from the critical temperature. If this is done, the agreement between the predicted critical enhancement and the experimental one is much better, as shown in Fig. 2. However, it is still clear that the measured enhancement is greater than the predicted one for the two isotherms closest to the critical temperature, although the deviation in the total viscosity of ethane does not exceed $\pm 1.3\%$. Even better agreement with the experimental data can be achieved if the critical temperature of the fluid, which was not measured by Iwasaki and Takahashi [43], is shifted by -0.1 K. However, there is no real justification for such a shift.

In any event, as shown later, the local background viscosity, which is suggested by the data of Iwasaki and Takahashi [43], is totally inconsistent with the behavior found from the analysis of all other primary data in the same density range, as argued in the next section and illustrated in Figs. 3 and 4. The conclusion is therefore inescapable that it is not possible to reconcile the experimental viscosity data of Iwasaki and Takahashi, within their estimated uncertainty, either with the data of other authors or with the predicted critical enhancement of the viscosity. This conclusion is analogous to that reached in the analysis of the results for carbon dioxide [2].

As a consequence of this analysis we prefer to represent the critical enhancement of the viscosity, $\Delta_c\eta$, of ethane by Eqs. (5), (7), and (8)

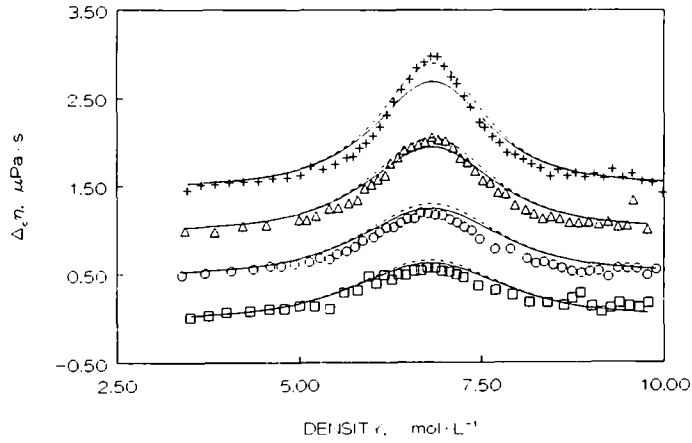

Fig. 2. The critical enhancement of the viscosity deduced from the data of Iwasaki and Takahashi [43] by the use of a "local" background viscosity: +, $T = 305.65$ K; △, $T = 305.85$ K; ○, $T = 306.15$ K; □, $T = 306.45$ K. The solid lines represent the values calculated from Eq. (5). The dashed lines represent the values calculated from Eq. (5) by reducing the value of the critical temperature by 0.1 K. To separate the isotherms the viscosity values have been displaced by 0.5 μPa·s each.

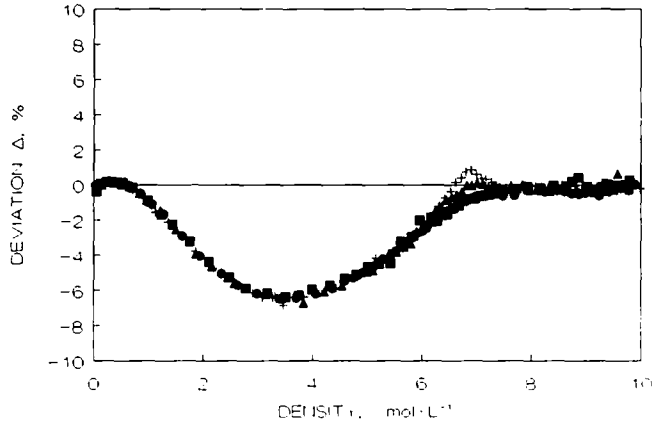

Fig. 3. Deviations, Δ, from the final excess correlation, Eq. (9), of the excess viscosity deduced from Iwasaki and Takahashi's data [43]: +, $T = 305.65$ K; ▲, $T = 305.85$ K; ●, $T = 306.15$ K; ■, $T = 306.45$ K. $\Delta = 100.0\ (\Delta\eta_{exp} - \Delta\eta_{cor})/\eta_{cor}$.

together with the relationships presented in Appendix II and the appropriate numerical coefficients given in Table II rather than to rely upon the experimental data. The equations should be used inside the region bounded approximately by 302.5 and 311 K in temperature and 4.3 and 8.6 mol · L^{-1} in density. Outside of this region the relative critical viscosity enhancement, $\Delta_c\eta/\eta$, is smaller than 1% and, for engineering purposes, can be safely neglected.

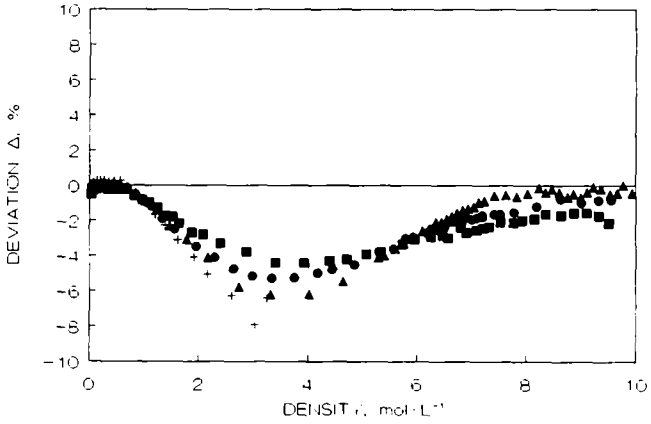

Fig. 4. Deviations, Δ, from the final excess correlation, Eq. (9), of the excess viscosity deduced from Iwasaki and Takahashi's data [43]: +, $T = 298$ K; ▲, $T = 308$ K; ●, $T = 323$ K; ■, $T = 348$ K. $\Delta = 100.0\ (\Delta\eta_{exp} - \Delta\eta_{cor})/\eta_{cor}$.

5. EXCESS VISCOSITY

The excess viscosity contribution describes how the viscosity of the pure fluid behaves as a function of density outside of the critical region. There is, as yet, no satisfactory theory for the excess viscosity over the whole of the phase space. It has been customary [2, 5, 7, 8, 13] to base the representations of the excess viscosity on a power series expansion in density of the form

$$\Delta\eta = \sum_{i=1}^{n} b_i \rho^i \tag{9}$$

where $b_i(T)$ are functions of temperature to be determined empirically. From observations on a number of fluids [13] it seems that, for supercritical temperatures, the coefficients b_i are often very weak functions of temperature. However, for the first coefficient b_1, recent theoretical work [11, 65–68] has established a temperature dependence which can be quite marked at subcritical temperatures. Indeed, the coefficient b_1 can change sign from positive to negative as the temperature is reduced. Thus, the viscosity in the vapor phase along an isotherm may first decrease owing to $b_1\rho$ and subsequently increase owing to the influence of higher-order terms as the density increases. This effect has been observed for a number of fluids [69, 70].

In order to obtain an accurate representation of the behavior of the viscosity in the vapor phase, the temperature dependence of the first density coefficient of viscosity must be taken into account. In principle, when experimental data in this range of densities are available, they can be used to determine $b_1(T)$. For ethane there are no suitable data available so that it is necessary to use theoretical predictions to determine this coefficient. We therefore depart from the usual practice [2] in this work and examine the initial dependence of the viscosity upon density separately from the behavior at higher densities.

5.1. Initial Density Dependence

As a result of both theoretical [11, 65–68] and experimental [10, 11, 71] studies of the first density coefficient of viscosity, it has been possible to develop a corresponding-states representation of its behavior which is extremely valuable. We therefore confine our attention now to densities such that only the term linear in density, $b_1\rho$, in Eq. (9) is significant. The coefficient b_1 can be written in terms of the second viscosity virial coefficient, B_η, by means of the definition

$$b_1(T) = B_\eta(T)\,\eta_0(T) \tag{10}$$

Following the assumption that a pure gas at low density can be modeled as a mixture of monomers and dimers, various contributions to the second viscosity virial coefficient can be identified

$$B_\eta = B_\eta^{(2)} + B_\eta^{(3)} + B_\eta^{(MD)} \tag{11}$$

Here $B_\eta^{(2)}$ is a contribution from two monomer collisions and $B_\eta^{(3)}$ is a contribution from three monomer collisions, while $B_\eta^{(MD)}$ is a contribution from monomer–dimer collisions. It has proved possible, by the use of a Lennard–Jones 12–6 potential, to calculate $B_\eta^{(2)}$ exactly [66, 68] and also to estimate contribution $B_\eta^{(3)}$ [65, 68]. Calculation of the monomer–dimer contribution $B_\eta^{(MD)}$ has also been performed [67, 68], but only under the assumption that the effective intermolecular potential for the monomer–dimer interaction is related to that of the monomer–monomer one by appropriate scaling. Under this assumption, and for small concentrations of dimers, a result for $B_\eta^{(MD)}$ is obtained which contains only two unknown parameters, δ and θ, both pertaining to the scaling of the monomer–dimer potential relative to that of the parent monomers.

The use of a single intermolecular pair potential, the Lennard–Jones 12–6, enables a comparison between experiment and theory to be conducted on the basis of the corresponding-states principle, so that the results for a number of gases have been expressed on a common basis. The most recent analysis [11] of this kind indicates that adoption of the values $\delta = 1.04$ and $\theta = 1.25$ leads to good agreement between the available data and the theoretical predictions. A particular advantage of the approach is that it is possible to evaluate the coefficient $B_\eta(T)$ for a gas for which no experimental viscosity data as a function of density exist given a knowledge only of the Lennard–Jones 12–6 parameters for the molecule. This procedure is valid only for the reduced temperature $T^* > 0.7$ ($T = 175$ K for ethane), because there are no experimental data at lower temperatures upon which to base the representation.

For the purposes of developing the present representation of the viscosity of ethane in the vapor phase, this lower limit will not be exceeded since the range of validity of the zero-density representation of the viscosity is $T = 200$ K. Nevertheless, experimental data in the liquid phase are available at much lower temperatures, extending to $T = 100$ K. In order to use a single overall viscosity correlation, given by Eq. (1), over the whole of the phase space, one has to ensure that the initial density dependence contribution extrapolates satisfactorily at low temperatures. For this purpose, for temperatures below $T^* = 0.7$, the second viscosity virial coefficient has been estimated by the use of the modified Enskog theory, which relates B_η to the second and third compressibility virial coefficients [72]. While

the procedure is rather crude, its limitations are of no practical significance in the liquid phase.

Although the method described above enables B_η to be evaluated, it is cumbersome for practical applications. Therefore B_η is written in the form

$$B_\eta = 0.6022137\sigma^3 B_\eta^*(T^*) \tag{12}$$

where the reduced second viscosity virial coefficient, B_η^*, is represented by a polynomial in reduced temperature of the form

$$B_\eta^* = \sum_{i=0}^{n} c_i / T^{*i} \tag{13}$$

where the reduced temperature is given by Eq. (4). The coefficients c_i are listed in Table III. Here B_η is in units of $\mathrm{L \cdot mol^{-1}}$ and σ is a characteristic length in nm. For the sake of consistency the scaling parameters ε and σ used in Eqs. (12) and (13) were chosen to coincide with those used for the zero-density viscosity representation. Equations (12) and (13), with the scaling coefficients ε and σ listed in Table I and the coefficients c_i in Table III, permit evaluation of the second viscosity virial coefficient B_η and thereby the initial density dependence of the viscosity [Eqs. (9) and (10)].

5.2. Density Dependence

In order to evaluate the higher density coefficients (b_i, $i = 2, n$) in Eq. (9) and thus develop the representation for the excess viscosity, it is necessary to resort to fitting the available primary experimental data. For this purpose Eq. (9) can be rewritten in terms of the first-density contribution and higher-density contributions, $\Delta_h \eta$, as

$$\Delta\eta = b_1 \rho + \Delta_h \eta = b_1 \rho + \sum_{i=2}^{n} b_i \rho^i \tag{14}$$

Table III. Coefficients for the Representation of the Initial Density Dependence of Ethane, Eq. (13)

i	c_i
0	−0.359 724 4
1	4.525 644
2	−5.474 280
3	3.396 994
4	−4.986 360
5	2.760 371
6	−0.682 778 9

where the higher-order density coefficients are most conveniently represented by the following functional form:

$$b_i = \sum_{j=0}^{m} e_{ij}/T^{*j}, \qquad i = 2, n \tag{15}$$

and where the reduced temperature is again given by Eq. (4), and the units of the coefficients e_{ij} are $(\mathrm{L} \cdot \mathrm{mol}^{-1})^i$.

There exist 14 sets of independent measurements [20, 22–25, 29, 32–36, 38, 43–46] of the viscosity of ethane at elevated pressures in the liquid or gaseous phases carried out over a period of 50 years in a number of different types of instruments. A critical review of all the available data has been carried out to establish the primary set. Only a small number of data fulfilled all of the requirements for primary data. Thus, in order to extend the range of the representation, a number of other sets of data have been included when it could be established that they were consistent with primary data in a region of overlap. In the process of data assessment a few rather large sets had to be classified as secondary. Two sets of measurements [25, 38] were carried out in instruments which do not conform to the criteria established for primary data and which covered a temperature and pressure range where more accurate data are available. Other measurements [22–24] were analyzed by the experimentalists in terms of simplistic working equations and, in any event, covered a limited range of temperatures at atmospheric pressure. The data of Meshcheryakov and Golubev [29], although measured by the use of a capillary viscometer, which is normally considered a primary instrument, showed large systematic deviations from the results of a number of other authors. The differences could not be reconciled without increasing the uncertainty of the final correlation by an unacceptable amount, so that these results were omitted from the primary data set. Figure A2 in Appendix III shows *a posteriori* the extent of the disagreement of this data set from our final correlation.

The data of Iwasaki and Takahashi [43] should, in principle, owing to the inherent precision and accuracy of their experimental technique, be treated as primary data and were used in this way in developing the viscosity correlation for carbon dioxide [2]. However, as noted earlier, their data are incompatible with those of other workers and two-thirds of the points fall within the critical region. To illustrate the difficulties, Fig. 3 shows the deviations of the viscosity along the four near-critical isotherms from the global correlation based on the excess function developed by the use of the results of other authors. The disagreement is very large and the deviations show a pronounced minimum, indicating a qualitatively different behavior of the excess. The analysis of the data of Iwasaki and Takahashi [43] farther away from the critical region has also been carried

out and Fig. 4 shows the deviations. Again, a pronounced minimum is observed in the deviation plot, supporting the claim that the excess function obtained from the data of Iwasaki and Takahashi [43], even far from the critical region, is markedly different from the excess function obtained from any other data. The results shown in Figs. 3 and 4 indicate that the estimated error in the viscosity of Iwasaki and Takahashi's data has to be increased by more than an order of magnitude to make it consistent with other results. For these reasons it was decided to classify all these data points as secondary.

The measurements of Diller and co-workers [44–46] have been carried out in an oscillating quartz-crystal viscometer, which does not satisfy the criteria of primary instrument because no complete working equation is available for it. Nevertheless, the majority of the data has been included in the primary set in order to increase the temperature and the pressure range covered and because they are consistent with other results. Only 40 points comprising all of the data determined in the gaseous phase [44, 45] have been classified as secondary and, as such, have been omitted from the fit. This is because the data were measured by the use of an instrument designed primarily for measurements in the liquid phase [44, 73]. In addition, these data show large deviations from the data of other authors as has been observed earlier for the supercritical viscosity data of carbon dioxide measured in the same instrument [2, 73].

The remaining data sets [32, 33, 35, 36, 44–46] have been classified as primary. Table IV lists all the experimental data chosen as primary, together with our estimates of their accuracy. The estimates of accuracy

Table IV. Primary Experimental Data for the Excess Viscosity of Ethane

Ref. No.	Method[a]	T (K)	P (MPa)	Phase[b]	Number of points	Ascribed accuracy (%)
Baron et al. [32]	C	325–408	0.7–55.1	S	40	2.0
Swift et al. [33]	FC	193–303	0.2–4.8	L	13	2.5
Eakin et al. [35]	C	298	4.5–55.1	L	16	1.5
Eakin et al. [35]	C	311–444	0.7–55.1	S	61	1.5
Carmichael & Sage [36]	RC	300–305	4.4–35.8	L	35	1.5
Carmichael & Sage [36]	RC	300–305	0.2–4.0	V	27	1.5
Carmichael & Sage [36]	RC	311–478	0.1–36.0	S	164	1.5
Diller & Saber [44, 45]	OQC	95–290	1.3–32.1	L	125	2.5
Diller & Ely [46]	OQC	295	7.6–51.9	L	8	2.5
Diller & Ely [46]	OQC	319–500	1.7–55.0	S	63	2.5

[a] FC, falling cylinder; C, capillary; RC, rotating cylinder; OQC, oscillating crystal.
[b] V, vapor; L, liquid; S, supercritical.

were based primarily on the authors' reported values, with some modifications where consistency checks or an examination of previous measurements with the same apparatus on other fluids implied larger uncertainty bands. Although some of the instruments used are capable of higher accuracy, the analysis carried out does not justify accuracies better than $\pm 1.5\%$ for any of the primary data sets.

Following the practice established for carbon dioxide [2], the excess viscosity has been determined for each datum by using Eq. (1) and subtracting the zero-density limit, η_0, and the critical enhancement, $\Delta_c\eta$, from the reported experimental value, η. In order to be consistent and minimize systematic errors in the individual measurements, we prefer to use η_0 reported by the experimentalists rather than the value obtained from Eq. (2). Unfortunately, only a few authors reported a η_0 value since, as can be seen from Table IV, the majority of measurements have been performed at pressures above 0.7 MPa. In order to estimate the "experimental" zero-density viscosity of each isotherm, we have, in the first instance, used values of η_0 and $b_1\rho$ obtained from Eqs. (2) and (10) to generate the first guess of the higher-density contribution to the excess viscosity, which was subsequently fitted to Eqs. (14) and (15). Equation (9) was then used to extrapolate the experimental data from the lowest pressure reported to zero and thus generate experimental zero-density viscosity values for each isotherm. Although this is not a strictly correct procedure, it ensures that all the experimental excess data tend to zero at zero density. Furthermore, the correction introduced by the extrapolation to zero pressure is small and, in general, does not exceed $\pm 0.5\%$.

In the next iteration the experimental zero-density viscosity and the viscosity critical enhancement estimated by the use of Eq. (5) have been used in Eq. (1) to obtain a new excess viscosity. Once the excess viscosity data have been generated, the initial density dependence is evaluated as $b_1\rho$ and subtracted from the excess to obtain the higher-density contribution, $\Delta_h\eta$. This quantity is then represented by Eqs. (14) and (15) to fit all of the available primary data. The fitting has been performed by the use of the SEEQ algorithm based on the stepwise least-squares technique [74]. The method requires initially a bank of power indices of temperature and density from which it chooses the statistically significant terms. The appropriate statistical weights have been generated from the experimental uncertainties given in Table IV for each data set and were taken to be inversely proportional to density. In order to achieve the best possible representation of the data, a further set of tests has been performed to examine any systematic deviations from the correlation. This process revealed that data of Eakin et al. [35] in the vapor phase along an isotherm at 298K exhibited systematic deviations with the maximum error

Table V. Coefficients for the Representation of the Excess Viscosity of Ethane Eqs. (14) and (15): $\Delta_h\eta = \sum_{i=2}^{6}\sum_{j=0}^{4} e_{ij}\rho^i/T^{*j}$

j	e_{2j}	$e_{3j}\times 10^1$	$e_{4j}\times 10^2$	$e_{5j}\times 10^3$	$e_{6j}\times 10^5$
0	0.717 837 04	0.133 030 49	0.0	0.0	0.0
1	−0.975 049 49	−3.933 419 9	1.941 579 4	0.0	0.0
2	0.0	8.148 111 2	−1.676 812 2	−2.663 598 7	7.749 540 2
3	1.157 371 9	−6.132 094 0	0.0	3.351 338 8	−9.783 933 4
4	0.0	0.0	1.527 033 9	−1.489 140 5	3.593 518 3

more than three times the estimated accuracy of the data. These data were eliminated from the primary set and thus have not been included in Table IV. The remainder of the primary data was refitted to Eqs. (14) and (15). The optimal values of coefficients e_{ij} are given in Table V. Figures 5–9 display the deviations of the primary experimental data for the viscosity of ethane from the representation developed here. The deviations shown in Figs. 5–9 have been plotted along isotherms to ascertain any systematic trends. No such trends have been observed and the excess correlation developed fits the data within ±2.0–2.5% or better over most of the phase space investigated.

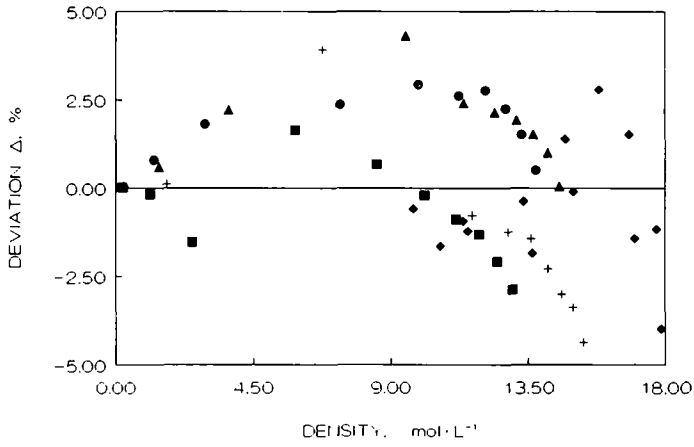

Fig. 5. Deviations, Δ, from the final excess correlation, Eq. (9), of the excess viscosity deduced from Baron et al. [32] and Swift et al. [33] data: +, $T = 325$ K [32]; ▲, $T = 353$ K [32]; ●, $T = 380$ K [32]; ■, $T = 408$ K [32]; ◆, Swift et al. [33]. $\Delta = 100.0\,(\Delta\eta_{exp} - \Delta\eta_{cor})/\eta_{cor}$.

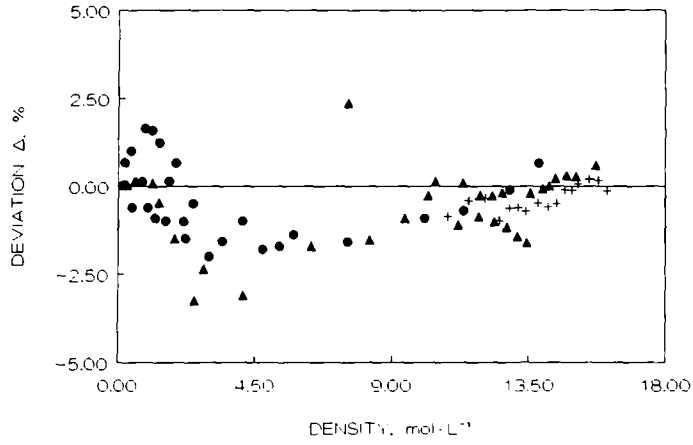

Fig. 6. Deviations, Δ, from the final excess correlation, Eq. (9), of the excess viscosity deduced from Eakin et al. data [35]: +, 298 K; ▲, T = 310–344 K; ●, T = 378–444 K. $\Delta = 100.0\ (\Delta\eta_{exp} - \Delta\eta_{cor})/\eta_{cor}$.

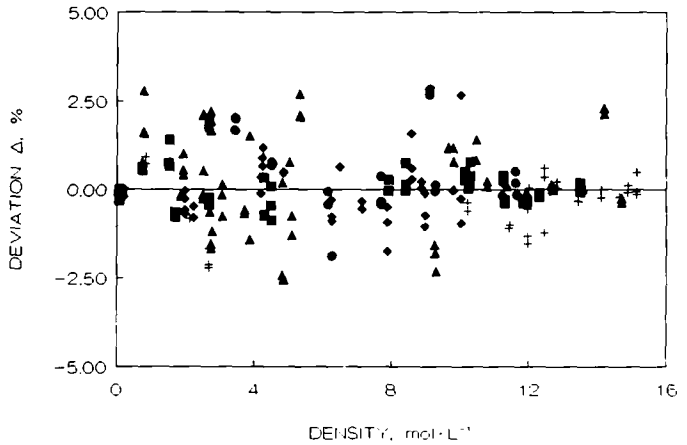

Fig. 7. Deviations, Δ, from the final excess correlation, Eq. (9), of the excess viscosity deduced from Carmichael et al. data [36]: +, T = 300 K; ▲, T = 305–310 K; ●, T = 327 K; ■, T = 344–377 K; ◆, T = 411–478 K. $\Delta = 100.0\ (\Delta\eta_{exp} - \Delta\eta_{cor})/\eta_{cor}$.

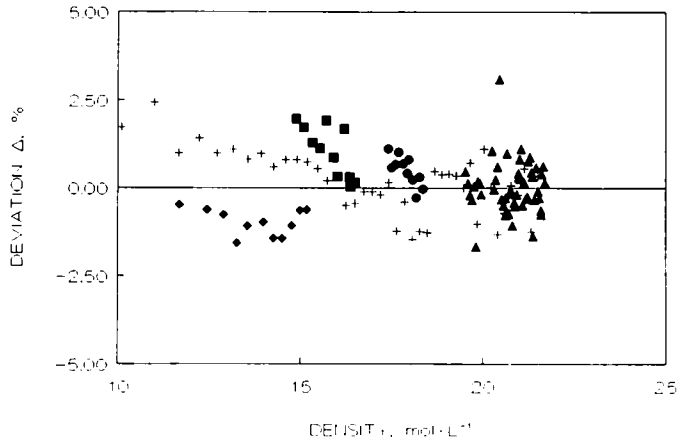

Fig. 8. Deviations, Δ, from the final excess correlation, Eq. (9), of the excess viscosity deduced from Diller and Saber's data [44, 45]: +, saturation line; ▲, $T = 100$–150 K; ●, $T = 200$ K; ■, $T = 250$ K; ◆, $T = 290$ K. $\Delta = 100.0\,(\Delta\eta_{exp} - \Delta\eta_{cor})/\eta_{cor}$.

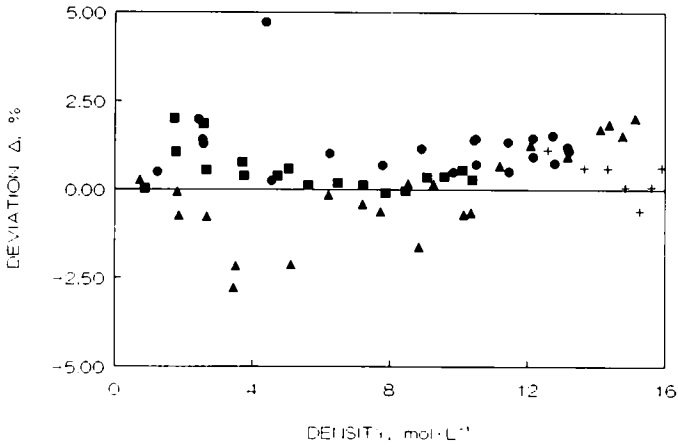

Fig. 9. Deviations, Δ, from the final excess correlation, Eq. (9), of the excess viscosity deduced from Diller and Ely's data [46]: +, $T = 295$ K; ▲, $T = 319$ K; ●, $T = 400$ K; ■, $T = 500$ K. $\Delta = 100.0\,(\Delta\eta_{exp} - \Delta\eta_{cor})/\eta_{cor}$.

6. THE OVERALL REPRESENTATION

The final representation of the viscosity of ethane is given by Eq. (1). The zero-density term, η_0, is given by Eqs. (2), (3), and (4) with the coefficients in Table I. The excess viscosity, $\Delta\eta$, is given by Eq. (14), where the coefficient b_1 is given by Eqs. (10), (12), and (13) with the coefficients in Table III. The coefficients b_i ($i = 2,..., n$) are given by Eq. (15) with the coefficients in Table V. The critical enhancement term, $\Delta_c\eta$, is given by Eq. (5) with the coefficients in Table II and the auxiliary equations defined in Appendix II. Appendix III contains a number of figures showing the deviations of the experimental viscosity data from that obtained by the use of the present correlation for the selected sets of data. Only primary data in the vapor and supercritical phase are shown in Fig. A1, since the final deviation plot for the primary data in the liquid is essentially the same as that in Fig. 8.

Figure 10 indicates the range of applicability of the present representation as well as the estimated uncertainty in various thermodynamic regions.

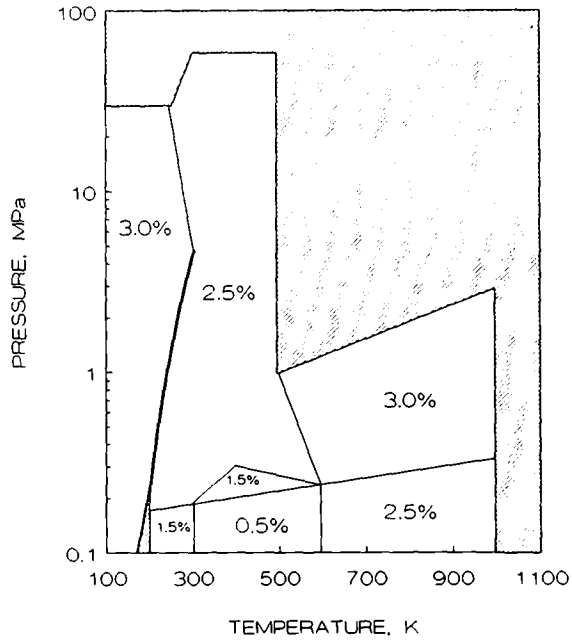

Fig. 10. The extent of the viscosity representation and its estimated uncertainty. No representation is available in the hatched region.

In the vapor phase and at low densities in the supercritical region, the correlation can be used between 200 and 1000 K. At higher densities in the supercritical region the upper temperature limit is lowered to 500 K owing to a lack of experimental data. Although the lower temperature limit in the gaseous phase is 200 K, the overall correlation can be used to estimate the liquid phase viscosities down to 100 K. The upper limit in pressure was set at 60 MPa. Any extrapolations to higher pressures can lead to a rapid reduction in the accuracy of the predicted viscosity and is not recommended.

In Appendix IV the viscosity of ethane along a number of isotherms as a function of pressure is tabulated in Table AII. Appendix V (Table AIII) contains the values of the viscosity along the saturation line. The values of viscosity in both appendices were generated directly from the representation given here by the use of EOS employed in this work as specified in Section 2. The values of viscosity as a function of temperature and density given in Appendix V can, in addition, be used to assist those programming the representative equations with checking of their coding.

7. DISCUSSION

As remarked earlier, a number of correlations have been proposed for the viscosity of ethane [3–8] in the past. In the interest of brevity a com-

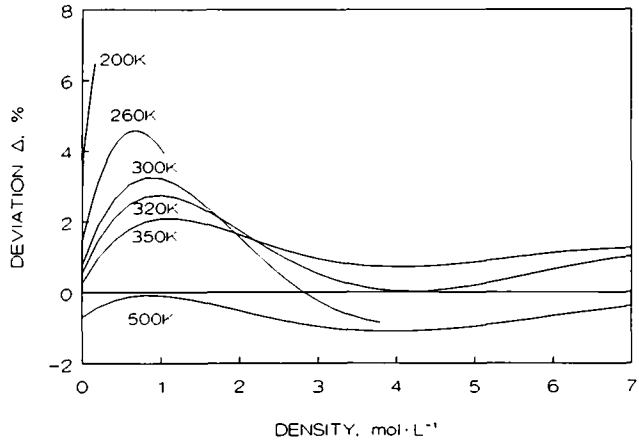

Fig. 11. Deviations, Δ, from the final correlation, Eq. (1), of the viscosity evaluated by the use of the Friend et al. correlation [8]. $\Delta = 100.0\ (\eta_{\mathrm{FIE}} - \eta_{\mathrm{cor}})/\eta_{\mathrm{cor}}$.

parison has been made only with the one most recently published [8] over the whole of the phase space. Figure 11 shows the deviations between the two representations along a number of selected isotherms. The isotherms were specifically chosen to be representative of the behavior in the vapor phase and at low densities, since it is here that the two correlations differ in their approach to the development of the representation. The inclusion of a new source of zero-density viscosity data at low temperatures [9] in the present work is seen to have a significant effect. The deviations at zero density between the two correlations increase with decreasing temperature, leading to an overestimate of the viscosity of ethane of 3% by the use of the correlation in Ref. 8 at 200 K. The results in Fig. 11 also show systematic deviations between the two correlations in the vapor phase. In this region there are no reliable experimental data, and whereas we based our correlation on the results of the theory of the initial density dependence, the correlation in Ref. 8 is based on equations fitted by the use of the supercritical and liquid viscosity data. Although the deviations shown in Fig. 11 are within the combined uncertainty ascribed to the correlations, we believe that in the vapor-phase region the present representation is an improvement on the previous one. In the supercritical and in the liquid phase, both correlations were based on the same set of

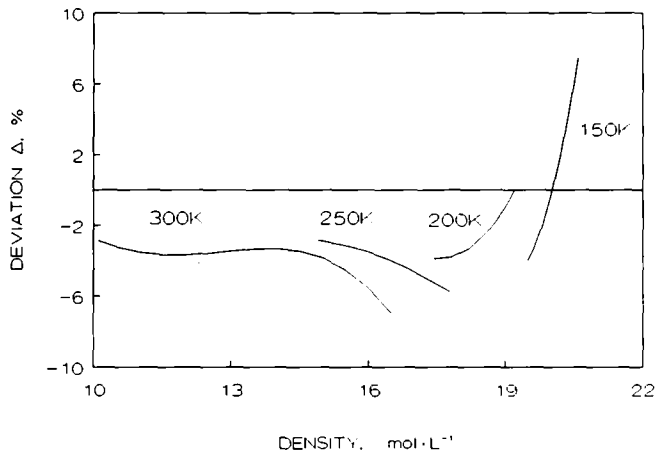

Fig. 12. Deviations, Δ, from the final correlation, Eq. (1), of the viscosity evaluated by the use of the Assael et al. [75] hard-sphere prediction scheme. $\Delta = 100.0\,(\eta_{HS} - \eta_{cor})/\eta_{cor}$.

experimental data so that it is not surprising to find that the deviations are small (of the order of $\pm 1.5\%$). In the critical region the present representation includes a term describing the critical enhancement of the viscosity omitted in the earlier work [8].

In developing the viscosity representation, no theoretical guidance has been used for the behavior of viscosity in the liquid phase. It is therefore interesting to compare the present correlation with the results of predictive schemes available in literature which have some theoretical foundation. For this purpose we have chosen the scheme developed by Assael et al. [75]. Their method is based on the hard-sphere theory of the transport properties of liquids. This theory indicates that among an entire series of similar molecules, the viscosity of the fluids can be reduced by means of just two system-dependent parameters to a single universal curve. One of the parameters is a characteristic volume, V_0, which is a weak function of temperature, while the other is a roughness factor R_η, a constant for the particular liquid. From the study of a wide range of fluids, representations of the universal function and of R_η and $V_0(T)$ have been developed which make possible the prediction of the viscosity of a particular liquid at a prescribed temperature and density with an estimated accuracy of $\pm 6\%$.

Figure 12 shows the deviations of the predicted viscosity from the values obtained by the use of the present correlation along four liquid-phase isotherms. Although systematic trends are observed which imply, at least for low temperatures, a density dependence different from that reported here, most of the deviations are within the accuracy claimed for the procedure.

8. CONCLUSION

The representation of the viscosity of ethane encompassing a large region of thermodynamic states has been presented. The formulation is based on a critical analysis of available experimental data guided by theoretical results. The uncertainty ascribed to the viscosity is nowhere greater than $\pm 3\%$, which for many engineering purposes will prove adequate. Nevertheless, it would be advantageous to have more measurements in the vapor phase, along the saturation line in the vapor phase, and in the immediate vicinity of the critical point in order to advance further our understanding of the behavior of the viscosity in these regions and also to decrease the ascribed uncertainties of the present correlation.

APPENDIX I

Table AI. List of All the Available Data from Measurements of the Viscosity of Ethane

Ref. No.	Method[a]	T (K)	P (MPa)	Phase[b]
15	OD	195–273	0.1	ZD
16	ODr	296	0.1	ZD
17	—	195–273	0.1	ZD
18	C	293–393	0.1	ZD
19	C	290–523	0.1	ZD
20	—	126–169	0.1	L
21	C	293–373	0.1	ZD
22	C	101–167	0.1	L
23	C	111–164	0.1	L
24	OC	173–288	0.1	L
25	RB	288–473	0.7–35	V, S, L
26	C	273	0.1	ZD
27	OP	308–351	0.1	ZD
28	—	303	0.1	ZD
29	C	258–523	0.1–81	ZD, V, S, L
30	OP	308–351	0.1	ZD
31	C	250–473	0.1	ZD
32	C	325–408	0.7–55	S
33	FC	193–303	0.2–48	L
34	C	302–311	4.4–5.9	V, S, L
35	C	298–444	0.7–55	V, S, L
36	RC	300–478	0.1–36	ZD, V, S, L
37	OD	296–304	0.1	ZD
38	OQC	305–322	4–6	S
39	C	305–408	0.1	ZD
40	C	373–673	0.1	ZD
41	OD	301–476	0.1	ZD
42	OD	298–468	0.1	ZD
43	OD	298–348	0.1–13	ZD, S
44, 45	OQC	95–320	0.6–32	V, S, L
46	OQC	295–500	1.7–55	S, L
9	C	213–393	0.1	ZD
10	OD	290–630	0.1	ZD

[a] FC, falling cylinder; C, capillary; RC, rotating cylinder; OD, oscillating disk; OQC, torsionally oscillating quartz crystal; ODr, oil drop; OC, oscillating cylinder; RB, rolling ball; OP, oscillating pendulum.

[b] ZD, zero density; V, vapor; L, liquid; S, supercritical.

APPENDIX II

Expressions for the Crossover Function H Entering the Description of the Critical Enhancement of the Viscosity, Eq. (5)

$$H(\{y_i\}) = h(\{y_i\}) + F(v_i, y_D) \sum_{i=1}^{3} \frac{(c_2 v_i^2 + c_1 v_i + c_0)}{\prod_{j=1, j\neq i}^{3} (v_i - v_j)} \tag{A1}$$

$$\begin{aligned} h(\{y_i\}) = {} & (3y_\gamma y_\eta + 1.5y_\eta - y_\eta^3 - y_v)\, y_D \\ & + (y_\eta^2 - 2y_\gamma - 5/4) \sin y_D - 0.25 y_\eta \sin 2y_D + (\sin 3y_D)/12 \\ & + \frac{[y_\gamma(1+y_\gamma)]^{3/2}}{(y_v - y_\gamma y_\eta)} \operatorname{arctg}\{[y_\gamma/(1+y_\gamma)]^{1/2} \operatorname{tg} y_D\} \end{aligned} \tag{A2}$$

$$\prod_{i=1}^{3} (v + v_i) = v^3 + y_\eta v^2 + y_\gamma v + y_v = 0 \tag{A3}$$

$$c_0 = y_\eta y_v (y_\eta^2 - 3y_\gamma - 2) + y_v^2 - y_\gamma y_v (1+y_\gamma)^2/(y_v - y_\gamma y_\eta) \tag{A4}$$

$$c_1 = (y_v - y_\gamma y_\eta)(y_\eta^2 - 3y_\gamma - 2) + y_\gamma^2 (1+y_\gamma)^2/(y_v - y_\gamma y_\eta) \tag{A5}$$

$$c_2 = y_\eta^4 - 2y_\eta^2(2y_\gamma + 1) + 2y_\eta y_v + 3y_\gamma^2 + 4y_\gamma + 1 \tag{A6}$$

Auxiliary functions

$$F(x, y_D) = \frac{1}{(1-x^2)^{1/2}} \ln \left[\frac{1 + x + (1-x^2)^{1/2} \operatorname{tg}(y_D/2)}{1 + x - (1-x^2)^{1/2} \operatorname{tg}(y_D/2)} \right] \tag{A7}$$

$$y_D = \operatorname{arctg}(q_D \xi) \tag{A8}$$

$$y_\delta = \frac{\operatorname{arctg}[q_D \xi/(1 + q_D^2 \xi^2)^{1/2}] - y_D}{(1 + q_D^2 \xi^2)^{1/2}} \tag{A9}$$

$$y_\alpha = 5.4935 \times 10^{-4} \frac{M \rho T}{\xi \bar{\eta}^2} \tag{A10}$$

$$y_\beta = \frac{M \bar{\lambda}}{(C_P - C_V)\bar{\eta}} \tag{A11}$$

$$y_\gamma = C_V/(C_P - C_V) \tag{A12}$$

$$y_\eta = (y_\delta + y_\beta/y_\alpha)/y_D \tag{A13}$$

$$y_v = y_\gamma y_\delta / y_D \tag{A14}$$

where T is temperature in Kelvin, ρ is density in $\text{mol} \cdot \text{L}^{-1}$, M is the relative molecular mass, $\bar{\eta}$ is the background viscosity in $\mu\text{Pa} \cdot \text{s}$, $\bar{\lambda}$ is the background thermal conductivity in $\text{mW} \cdot \text{m}^{-1} \cdot \text{K}^{-1}$, C_P and C_V are isobaric and

isochoric molar heat capacities, respectively, in $J \cdot mol^{-1} \cdot K^{-1}$, ξ is a correlation length in nm, and q_D is a large wave-number cutoff parameter in nm^{-1}.

The thermodynamic functions C_P and C_V and ξ, which is related to the compressibility through Eq. (7), are to be calculated from the EOS as specified in Section 2. The background viscosity, $\bar{\eta}$, is given by

$$\bar{\eta}(\rho, T) = \eta_0(T) + \Delta\eta(\rho, T) \tag{A15}$$

with $\eta_0(T)$ calculated from Eq. (2) and $\Delta\eta(\rho, T)$ from Eq. (14). The background thermal conductivity, $\bar{\lambda}$, is given by

$$\bar{\lambda}(\rho, T) = \lambda_0(T) + \Delta\lambda(\rho, T) \tag{A16}$$

with the dilute gas thermal conductivity, $\lambda_0(T)$, and the excess thermal conductivity, $\Delta\lambda(\rho, T)$, to be calculated as specified in part II [76].

APPENDIX III

Deviation Plots of the Selected Experimental Data from the Correlation

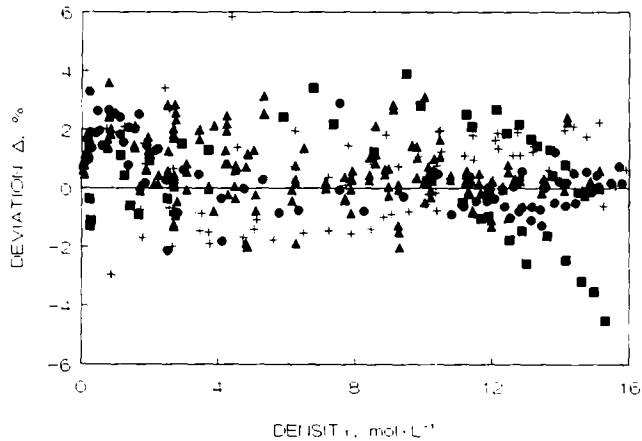

Fig. A1. Deviations, Δ, from the final correlation, Eq. (1), of the primary viscosity data in the vapor and supercritical regions: + [46]; ▲ [36]; ● [35]; ■ [32]. $\Delta = 100.0\,(\eta_{exp} - \eta_{cor})/\eta_{cor}$.

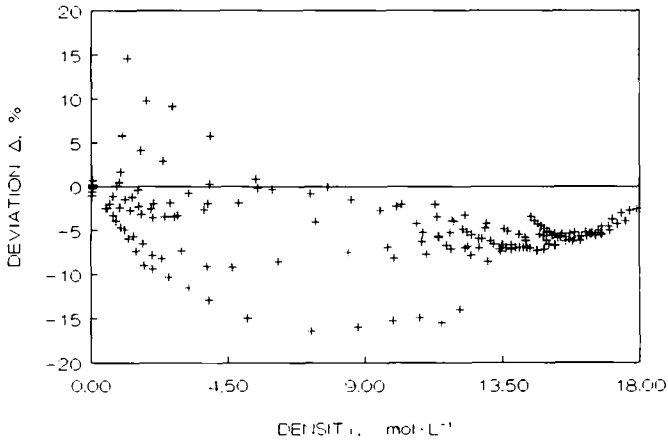

Fig. A2. Deviations, Δ, from the final correlation, Eq. (1), of the viscosity data of Meshcheryakov and Golubev [29]. $\Delta = 100.0\,(\eta_{exp} - \eta_{cor})/\eta_{cor}$.

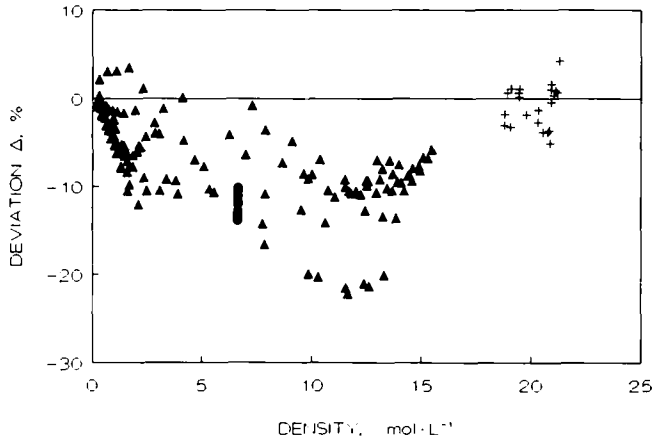

Fig. A3. Deviations, Δ, from the final correlation, Eq. (1), of the selected secondary viscosity data: ▲ [25]; + [22, 23]; ● [38]. $\Delta = 100.0\,(\eta_{exp} - \eta_{cor})/\eta_{cor}$.

APPENDIX IV

Table AII. Tabulation of the Viscosity of Ethane

	Viscosity of ethane η (μPa · s) at T (K)											
P (MPa)	100	150	200	250	275	300	306	310	350	400	450	500
0.10	878.0	271.8	6.08	7.74	8.54	9.31	9.49	9.61	10.80	12.22	13.58	14.88
0.50	881.2	272.7	137.25	7.71	8.53	9.33	9.51	9.64	10.84	12.27	13.63	14.93
1.00	885.3	273.7	138.04	7.80	8.60	9.40	9.58	9.71	10.91	12.35	13.71	15.01
2.00	893.3	275.9	139.59	78.13	9.13	9.75	9.92	10.03	11.17	12.57	13.91	15.20
3.00	901.4	278.0	141.12	79.77	57.59	10.53	10.61	10.67	11.57	12.88	14.17	15.43
5.00	917.4	282.2	144.13	82.88	61.74	39.36	28.11	15.11	12.99	13.76	14.87	16.02
8.00	941.4	288.4	148.51	87.20	66.89	48.96	44.61	41.64	17.97	15.85	16.31	17.18
10.00	957.4	292.4	151.36	89.91	69.90	53.01	49.18	46.65	24.18	17.82	17.52	18.10
20.00	1037.1	312.1	164.77	102.02	82.42	67.03	63.81	61.74	44.46	31.12	25.68	24.00
30.00	1116.3	330.6	177.13	112.63	92.75	77.42	74.25	72.23	55.57	41.90	34.28	30.63
40.00	—	—	—	—	101.97	86.37	83.16	81.12	64.34	50.35	41.82	37.01
50.00	—	—	—	—	—	94.51	91.23	89.15	72.02	57.64	48.52	42.96
60.00	—	—	—	—	—	102.12	98.77	96.63	79.09	64.26	54.66	48.55

APPENDIX V

Table AIII. Viscosity of Ethane Along the Saturation Line

T (K)	P (MPa)	$\rho_{vap.}$ (mol·L^{-1})	$\eta_{vap.}$ (μPa·s)	$\rho_{liq.}$ (mol·L^{-1})	$\eta_{liq.}$ (μPa·s)
100.0	1.1×10^{-5}	1.3×10^{-5}	—	21.323	876.02
120.0	3.55×10^{-4}	3.56×10^{-4}	—	20.597	486.51
140.0	3.83×10^{-3}	3.30×10^{-3}	—	19.852	322.16
160.0	0.02145	0.01631	—	19.081	232.45
180.0	0.07872	0.05412	—	18.276	175.74
200.0	0.2174	0.1387	6.020	17.423	136.73
220.0	0.4923	0.3001	6.684	16.498	108.24
230.0	0.7005	0.4221	7.055	15.999	96.62
240.0	0.9671	0.5810	7.472	15.467	86.27
250.0	1.3012	0.7867	7.958	14.892	76.91
260.0	1.7120	1.0534	8.544	14.261	68.29
270.0	2.2097	1.4038	9.278	13.551	60.17
280.0	2.8058	1.8787	10.25	12.723	52.28
290.0	3.5144	2.5703	11.64	11.683	44.19
295.0	3.9169	3.0723	12.67	11.010	39.77
300.0	4.3560	3.8129	14.23	10.101	34.63
302.0	4.5432	4.2616	15.23	9.5867	32.09
304.0	4.7377	4.9547	16.91	8.8412	28.85

ACKNOWLEDGMENTS

Financial support for the IUPAC Transport Properties Project Center at Imperial College is provided by the U.K. Department of Trade and Industry. The research at the University of Maryland is supported by the Division of Chemical Sciences of the Office of Basic Energy Sciences of the U.S. Department of Energy under Grant DE-FG05-88ER-13902. The collaboration between Imperial College and University of Maryland is supported by NATO Research Grant 0008/88, and the collaboration with the Universities of Rostock and Thessaloniki is supported by the British Council and Deutscher Akademischer Austauschdienst, while that between the University of Rostock and the University of Thessaloniki was part of the Greek–German Agreement on Scientific Cooperation. This work was carried out under the auspices of the Subcommittee on Transport Properties of Commission I.2 of the International Union of Pure and Applied Chemistry.

REFERENCES

1. M. J. Assael, C. A. Nieto de Castro, and W. A. Wakeham, *Chem. Por.* **78**:16.1 (1978).
2. V. Vesovic, W. A. Wakeham, G. A. Olchowy, J. V. Sengers, J. T. R. Watson, and J. Millat, *J. Phys. Chem. Ref. Data* **19**:763 (1990).
3. I. F. Golubev, *The Viscosity of Gases and Gas Mixtures* (Israel Program for Scientific Translations, Jerusalem, 1970).
4. T. Makita, Y. Tanaka, and A. Nagashima, *Rev. Phys. Chem. (Jap.)* **44**:98 (1974).
5. H. J. M. Hanley, K. E. Gubbins, and S. Murad, *J. Phys. Chem. Ref. Data* **6**:1167 (1977).
6. A. A. Tarzimanov, V. E. Lyusternik, and V. A. Arslanov, *Viscosity of Gaseous Hydrocarbons, a Survey of Thermophysical Properties of Compounds, No. 1 (63)* (Institute of High Temperatures, Moscow, 1987).
7. B. A. Younglove and J. F. Ely, *J. Phys. Chem. Ref. Data* **16**:577 (1987).
8. D. G. Friend, H. Ingham, and J. F. Ely, *J. Phys. Chem. Ref. Data* **20**:275 (1991).
9. I. Hunter and E. B. Smith, personal communication (1989).
10. S. Hendl and E. Vogel, *Fluid Phase Equil.* **76**:259 (1992).
11. E. Bich and E. Vogel, *Int. J. Thermophys.* **12**:27 (1991).
12. J. Luettmer-Strathmann, S. Tang, and J. V. Sengers, *J. Chem. Phys.* **97**:2705 (1992).
13. V. Vesovic and W. A. Wakeham, in *Critical Fluid Technology*, T. J. Bruno and J. F. Ely, eds. (CRC Press, Boca Raton, FL, 1991), Chap. 6.
14. R. Mostert, H. R. van den Berg, P. S. van der Gulik, and J. V. Sengers, *J. Chem. Phys.* **92**:5454 (1990).
15. H. Vogel, *Ann. Phys.* **43**:1235 (1914).
16. Y. Ishida, *Phys. Rev.* **21**:550 (1923).
17. G. Martin, *A Treatise on Chemical Engineering* (Lockwood and Son, London, 1928).
18. T. Titani, *Bull. Chem. Soc. (Jap.)* **5**:98 (1930).
19. M. Trautz and K. G. Sorg, *Ann. Phys.* **10**:81 (1931).
20. N. S. Rudenko and L. W. Schubnikow, *Phys. Z. Sowjetunion* **6**:470 (1934) [data quoted by A. Van Itterbeek and O. van Paemel, *Physica* **8**:133 (1941)].
21. H. Adzumi, *Bull. Chem. Soc. (Jap.)* **12**:199 (1937).
22. S. F. Gerf and G. I. Galkov, *Zhur. Tekh. Fiz.* **10**:725 (1940).
23. G. I. Galkov and S. F. Gerf, *Zhur. Tekh. Fiz.* **11**:613 (1941).
24. S. F. Gerf and G. I. Galkov, *Zhur. Tekh. Fiz.* **11**:801 (1941).
25. A. S. Smith and G. G. Brown, *Ind. Eng. Chem.* **35**:705 (1943).
26. V. D. Majmudar and V. S. Oka, *J. Univ. Bombay* **17A**:35 (1949).
27. P. M. Craven and J. D. Lambert, *Proc. Roy. Soc. (London)* **205A**:439 (1951).
28. H. Senftleben, *Z. Angew. Phys.* **5**:33 (1953).
29. N. V. Meshcheryakov and I. F. Golubev, *Trudy GIAP* **4**:22 (1954).
30. J. D. Lambert, K. J. Cotton, M. W. Pailthorpe, A. M. Robinson, J. Scrivins, W. R. F. Vale, and R. M. Young, *Proc. Roy. Soc. (London)* **231A**:280 (1955).
31. A. G. DeRocco and J. O. Halford, *J. Chem. Phys.* **28**:1152 (1958).
32. J. D. Baron, J. G. Roof, and F. W. Wells, *J. Chem. Eng. Data* **4**:283 (1959).
33. G. W. Swift, J. Lohrenz, and F. Kurata, *AIChE J.* **6**:415 (1960).
34. K. E. Starling, B. E. Eakin, J. P. Dolan, and R. T. Ellington, *Proc. 2nd Symp. Thermophys. Prop.*, P. F. Masi and D. H. Tsai, eds. (American Society of Mechanical Engineers, New York, 1962), p. 530.
35. B. E. Eakin, K. E. Starling, J. P. Dolan, and R. T. Ellington, *J. Chem. Eng. Data* 7:33 (1962); ADI Document No. 6856.
36. L. T. Carmichael and B. H. Sage, *J. Chem. Eng. Data* **8**:94 (1963).
37. J. Kestin, S. T. Ro, and W. A. Wakeham, *Trans. Faraday Soc.* **67**:2308 (1971).

38. H. J. Strumpf, A. F. Collings, and C. J. Pings, *J. Chem. Phys.* **60**:3109 (1974).
39. M. Diaz Pena and J. A. R. Cheda, *Anales Quim. (Espana)* **71**:34 (1975).
40. A. Cabello, F. Pedrosa, and M. Diaz Pena, *Anales Quim. (Espana)* **73**:37 (1977).
41. J. Kestin, H. E. Khalifa, and W. A. Wakeham, *J. Chem. Phys.* **66**:1132 (1977).
42. Y. Abe, J. Kestin, H. E. Khalifa, and W. A. Wakeham, *Physica* **93A**:155 (1978).
43. H. Iwasaki and M. Takahashi, *J. Chem. Phys.* **74**:1930 (1981).
44. D. E. Diller and J. M. Saber, *Physica* **108A**:143 (1981).
45. D. E. Diller, *Proc. 8th Symp. Thermophys. Prop.*, J. V. Sengers, ed. (American Society of Mechanical Engineers, New York, 1982), Vol. I, p. 219.
46. D. E. Diller and J. F. Ely, *High Temp. High Press.* **21**:613 (1989).
47. R. D. Trengove and W. A. Wakeham, *J. Phys. Chem. Ref. Data* **16**:175 (1987).
48. J. Millat, V. Vesovic, and W. A. Wakeham, *Int. J. Thermophys.* **12**:265 (1991).
49. G. C. Maitland, M. Rigby, E. B. Smith, and W. A. Wakeham, *Intermolecular Forces: Their Origin and Determination* (Clarendon Press, Oxford, 1987).
50. S. Hendl, J. Millat, V. Vesovic, E. Vogel, and W. A. Wakeham, *Int. J. Thermophys.* **12**:999 (1991).
51. CODATA Bulletin No. 63 (1986).
52. E. Bich, J. Millat, and E. Vogel, *Wiss. Z. W.-Pieck-Univ. Rostock* **36**(N8):5 (1987).
53. A. Boushehri, J. Bzowski, J. Kestin, and E. A. Mason, *J. Phys. Chem. Ref. Data* **16**:445 (1987); **17**:255 (1988).
54. J. V. Sengers, *Int. J. Thermophys.* **6**:203 (1985).
55. S. L. Rivkin, A. Ya. Levin, L. B. Izrailevsky, and K. G. Kharitonov, *Proc. 8th Int. Conf. Prop. Steam*, P. Bury, H. Perdon, and B. Vodar, eds. (Editions Européennes Thermiques et Industries, Paris, 1975), p. 153.
56. R. S. Basu, J. V. Sengers, and J. T. R. Watson, *Int. J. Thermophys.* **1**:33 (1980).
57. V. N. Zozulya and Y. P. Blagoi, *Sov. Phys. JETP* **39**:99 (1974).
58. R. F. Berg and M. R. Moldover, *Phys. Rev.* **A42**:7183 (1990).
59. R. F. Berg and M. R. Moldover, *J. Chem. Phys.* **93**:1926 (1990).
60. G. A. Olchowy and J. V. Sengers, *Phys. Rev. Lett.* **61**:15 (1988).
61. R. Kraus, J. Luettmer-Strathmann, J. V. Sengers, and K. Stephan, *Int. J. Thermophys.* **14**:951 (1993).
62. R. F. Berg and M. R. Moldover, *J. Chem. Phys.* **89**:3694 (1988).
63. J. C. Nieuwoudt and J. V. Sengers, *J. Chem. Phys.* **92**:5454 (1990).
64. H. Hao and R. A. Ferrell, in press.
65. D. G. Friend, *J. Chem. Phys.* **79**:4533 (1983).
66. J. C. Rainwater, *J. Chem. Phys.* **81**:495 (1984).
67. D. G. Friend and J. C. Rainwater, *Chem. Phys. Lett.* **107**:590 (1984).
68. J. C. Rainwater and D. G. Friend, *Phys. Rev.* **A36**:4062 (1987).
69. M. Takahashi, C. Yokoyama, and S. Takahashi, *Kagaku Kogaku Ronbunshu* **11**:155 (1985).
70. M. Takahashi, C. Yokoyama, and S. Takahashi, *J. Chem. Eng. Data* **32**:98 (1987).
71. E. Vogel and S. Hendl, *Fluid Phase Equil.* **79**:313 (1992).
72. H. J. M. Hanley, R. D. McCarty, and E. G. D. Cohen, *Physica* **60**:322 (1972).
73. D. E. Diller and M. J. Ball, *Int. J. Thermophys.* **6**:619 (1985).
74. K. M. de Reuck and B. Armstrong, *Cryogenics* **19**:505 (1979).
75. M. J. Assael, E. Charitidou, J. H. Dymond, and M. Papadaki, *Int. J. Thermophys.* **13**:237 (1992).
76. V. Vesovic, W. A. Wakeham, J. Luettmer-Strathmann, J. V. Sengers, J. Millat, E. Vogel, and M. J. Assael, *Int. J. Thermophys.* **15**:33 (1994).